EXPERIMENTAL PETROLOGY AND ORIGIN OF FRA MAURO ROCKS AND SOIL

David Walker, John Longhi, and James Fred Hays
Department of Geological Sciences, Harvard University
Cambridge, Massachusetts 02138

ABSTRACT

Melting experiments over the pressure range 0 to 20 kilobars on Apollo 14 igneous rocks 14310 and 14072 and on comprehensive fines 14259 demonstrate the following:

1) Low pressure crystallization of rocks 14310 and 14072 proceeds as predicted from the textural relationships displayed by thin sections of these rocks. The mineralogy and textures of these rocks are the result of near surface crystallization.

2) The chemical compositions of these lunar samples all show special relationships to multiply saturated liquids in the system: anorthite-forsterite-fayalite-silica at low pressure.

3) Partial melting of a lunar crust consisting largely of plagioclase, low calcium pyroxene, and olivine, followed by crystal fractionation at the lunar surface is a satisfactory mechanism for the production of the igneous rocks and soil glasses sampled by Apollo 14. The KREEP component of other lunar soils may have a similar origin.

CONTENTS

INTRODUCTION

The Apollo 14 mission to the Fra Mauro Hills of the moon in the spring of 1971 returned many breccias which have geological significance in establishing by close-up observation the clastic nature of the Fra Mauro formation which had been previously inferred from remote observation. Few of the rocks returned have textures that can reasonably be interpreted as resulting from the direct crystallization of a silicate melt; however, many of the breccia clasts have igneous textures. Rock 14310 is a 3.4 kg rock that has been widely interpreted as igneous. Rock 14072 is a 45 g fragment that also appears to be igneous. Interpretation of the magmatic history of these rocks, apart from their subsequent mechanical adventures, may lead to a better understanding of lunar volcanic processes and the nature of the pre-Imbrian lunar crust, and may ultimately help to place constraints on the constitution and origin of the moon.

Our petrographic observations of polished thin sections 14310,30 and 14072,16 (Longhi, Walker and Hays, 1972) coupled with phase equilibrium experiments on a homogenized powder sample 14310,138, a powdered rock chip 14072,3, and a

sample of comprehensive fines 14259,85 have led to a successful reconstruction of the near-surface volcanism that produced the Apollo 14 igneous rocks. Consideration of the chemical compositions and phase relations of these and other lunar materials suggest a model for the nature of the lunar crust and for the production of silicate melts capable of yielding crystalline rocks such as those of the Fra Mauro formation. The origin of the KREEP component of lunar fines is also explained by our model.

EXPERIMENTAL PROCEDURES

About one gram of each sample studied was finely ground under acetone in an agate mortar for 20 minutes. The resulting powder of grain size less than 40 microns was stored in a stoppered glass vial in a dessicator. Approximately 2 mg of powder was used in each run. This powder consisted largely of the crystalline material of the original rock or soil plus the small percentage of glass also there. The homogeneity of the starting material was monitored by analysis of runs above the liquidus with an electron microprobe. Crystalline starting material was employed to avoid the changes in oxidation state inherent in preliminary fusions. This procedure has two extra benefits: 1) nucleation of phases present is no problem; 2) at temperatures well below the liquidus, crystals remain of size large enough for microprobe analysis. It is possible that experimental products might be biased in favor of the starting materials when using crystalline powders. To avoid such a possibility and to demonstrate the equilibrium nature of our products, some runs were equilibrated above the liquidus and then dropped to a lower temperature. In this manner several important phase boundaries

on the P, T diagram were reversed. We had less success in reversing the liquidus at high pressures than at low pressure where we were generally successful, no doubt a result of the longer run times.

Work done at low pressure was performed in molybdenum capsules. These capsules were drilled from 2.54 mm molybdenum rod and had friction fitted molybdenum stoppers to contain the charges. The capsules were sealed in evacuated silica glass tubes. While the glass was being evacuated the sample was gently heated with an oxygen-hydrogen torch to dry it and then the sample was sealed off under vacuum. The sealed silica glass vessels were then suspended at the hot spot of a vertical tube platinum-wound quenching furnace less than 5 mm from a Pt-Pt10Rh thermocouple junction. Temperature control was maintained by monitoring this thermocouple and adjusting the furnace power for temperature deviations from the desired temperature. The control is precise to ± 1/3°C over periods of weeks. Quenching was accomplished by dropping the silica glass vessel out the bottom of the furnace into a dish of water. Quenching times were less than 2 seconds. Run times varied from 4 hours to 5 days in length.

Our thermocouples were calibrated against the melting points of gold (1064.5°C) and lithium metasilicate (1203°C). The assembly of silica tube and thermocouple was the same as during a quenching run. The calibration material was held at successively higher temperatures until melting was observed. Melting intervals were less than a degree. The corrections to normal thermocouple EMF/temperature tables were between 3 and 15 degrees depending on the age of the thermocouple and the length of use above 1300°C.

Experiments conducted at high pressure were performed in a solid-medium, piston-cylinder apparatus (Boyd and England, 1960, 1963). Capsules drilled from molybdenum rod were used to contain the sample. Furnace assembly, capsule, and sample were dried in dry nitrogen at 1100°C for one half hour. Boron nitride was used as a sleeve and Pt-Pt10Rh was used as a thermocouple pair. All runs were carried out on piston-in strokes with a -8% friction correction being applied to the nominal pressure to determine the pressure of the run (Johannes et. al,, 1971). The pressure was raised before the internal graphite resistance furnace was heated, but the final piston-in pressure adjustment was made at run temperature. No correction was made for the effect of pressure on thermo-

couple EMF and the thermocouples were not individually calibrated. Quenching was carried out by turning off the furnace power. Quenching times were less than ten seconds. Before quenching, temperature control was maintained to ± 2°C by monitoring the thermocouple EMF and correcting the furnace power for temperature fluctuation. Run lengths could not profitably be made longer than a day due to thermocouple contamination. Increasing degrees of melting were observed in products equilibrated for longer periods of time at constant thermocouple EMF. Both vitreous and crystalline starting materials give this result so the effect cannot be kinetic. Platinum and alumina discs were placed between the thermocouple junction and the sample capsule to protect against contamination from below. Either this precaution was ineffective or the contamination comes from elsewhere (cf. Mao and Bell, 1971).

Capsule material and oxidation states

Equilibrium studies on iron bearing silicate systems suffer from difficulties introduced by the variable oxidation state of iron. In the lunar samples very little, if any, Fe^{+3} is observed whereas native iron metal is commonly present

with ferrous silicates. Experiments conducted under oxidizing conditions would not properly model the lunar environment of crystallization. It is difficult to find an ideal container on which to conduct experiments under reducing conditions. Platinum has long been known to remove iron metal from the sample, changing the total iron content and oxidation state of the remaining iron. Using a platinum capsule resulted in replacement of liquidus plagioclase by spinel in 14310 and changed the color of the glass from green to brown. Graphite which might be satisfactory at high pressures, were it not for its lack of mechanical integrity, is totally unsatisfactory at low pressure where smelting occurs. Any ferrous iron reacts with the graphite to produce metal and carbon monoxide which bursts the silica tube. Other laboratories have used iron capsules. If the starting material is in a somewhat oxidized state, reaction with the metal container enriches the melt in FeO and may cause leaks in the container. If the starting material is reduced we observed rather erratic concentrations of iron in the melt in runs of less than 10 hours. We have used molybdenum as a capsule material. Our investigations into the diffusion of iron into molybdenum

have shown that the alloy Fe_3Mo_2 might be a better capsule material. The commercial unavailability of this material prevents its use at this time. The high melting temperature of molybdenum and the low diffusion coefficient of iron into molybdenum (Walker and Hays, 1972) in the temperature range of the experiments have prompted the use of molybdenum as a reasonable alternative.

Our experimental conditions, sealed tubes and piston-cylinder apparatus, allow the oxidation state of the iron in the charge to vary only by interaction with the molybdenum, Rock 14310 and the homogeneous starting powder contain some metallic iron as part of the total iron reported as FeO in published analyses (Ringwood and Green, 1972; Kushiro, 1972). Low pressure runs in molybdenum above the liquidus do not show iron droplets but electron probe analysis of the glass shows that about half the "FeO" reported in whole-rock analyses is gone. This iron is found in the molybdenum capsules. Long runs in iron capsules however show the same amount of iron "loss" suggesting that immiscibility of the reduced fraction of the iron is responsible for the low FeO content of the melts rather than the extraction of ferrous iron by the molybdenum capsule. Long runs in molybdenum do not decrease FeO in the liquid significantly below the level reached in long runs in iron capsules under these closed capsule conditions. It is only the metallic iron droplets

which have been removed by the molybdenum during the long runs. Figure 1 shows the results of analyses of glasses formed by equilibrating sample charges at temperatures just above liquidus. A pressure of 5 kb on the liquid in a graphite capsule was apparently sufficient to dissolve the metallic iron since the analysis of this run has a full complement of iron in the silicate glass. The diagram shows that the low pressure glasses in molybdenum and in iron have less iron than the whole rock value. (Iron plots at ferrosilite in this diagram.) It is also evident that short runs in iron capsules give erratic results for unknown reasons but all differ from the whole rock in having too little iron in the glass. We may conclude that for low pressures the molybdenum capsule in a sealed silica tube holds the oxidation state of the charge constant. The capsule is self buffered. We shall see that in the case of 14310 this was perhaps not the most desirable circumstance since the rock suffered substantial sub-solidus reduction later than the events of the main crystallization.

The control of oxidation state at high pressures appears to be maintained either internally or by the capsule depending on temperature. Two regions on our pressure-

temperature diagram could be distinguished on the basis of whether MoO_2 or iron metal droplets (short runs) were present in the experimental product. The production of MoO_2 in a closed system requires a reaction of the sort

$$2FeO(\text{sample}) + 21Mo(\text{capsule}) = Fe_2Mo_{20}(ss) + MoO_2(xtl)$$

Biggar's (1970) data suggests that the Mo-MoO_2 buffer is rather close to the Fe-FeO buffer in the temperature range of our experiments. The fact that iron metal, which is present in the starting material disappears in some cases cannot be an oxidation effect because the iron content of the glass actually decreases. The fact that at the same time the iron metal disappears, presumably by diffusion into the molybdenum, we observe MoO_2 to appear implies that some reduction of the FeO is occurring by the above reaction. This in turn implies that the f_{O_2} (T,P) buffer curve for Mo-MoO_2 must lie below the Fe-FeO equilibrium in our charge, at least for temperatures above which diffusion becomes significant. The removal of the iron metal phase is not a serious problem since its only practical effect when present was to buffer f_{O_2}. This function is assumed by the molybdenum. The fact that molybdenum is able to reduce FeO by dissolving iron is analogous to the platinum problem. We are somewhat better off with molybdenum

since the remaining iron is not oxidized but instead the Mo forms MoO_2. Then the only detrimental effect is the change in FeO content of the liquid caused by the slightly greater reducing power of Mo than Fe. The amount of MoO_2 produced is quite small so this effect is thought to be unimportant. We may conclude that at temperatures sufficient for significant diffusion, oxidation state is controlled by Mo-MoO_2 reducing FeO. At lower temperatures the charge is self buffered.

RESULTS OF CRYSTALLIZATION EXPERIMENTS

The products and conditions of our experimental runs are given in Table 1. The full pressure-temperature diagrams for the compositions studied are given in Figures 2, 3, and 4. The results of our crystallization experiments in sealed silica tubes are summarized in Figure 5.

The low pressure crystallization of sample 14310,138 begins with plagioclase (An 92) precipitating at 1310°C and precipitating alone until 1202°C where both orthopyroxene (En 88, Wo 3) and a trace of olivine (Fo 89) appear. Olivine disappears very quickly below 1200°C and at 1190°C the orthopyroxene has begun to react with the liquid to produce pigeonite (En 86, Wo 5). At 1100°C a silica phase, probably tridymite, is present in the residuum. With increasing pressure plagioclase remains the liquidus phase up to 10 kb; however, olivine and orthopyroxene are replaced by pigeonite as the primary ferromagnesian mineral in this pressure range. In the neighborhood of 15 kb spinel and possibly aluminous orthopyroxene are on the liquidus. At about 12 kb pigeonite must be very nearly on the liquidus and at about 18 kb aluminous clinopyroxene must be near the liquidus.

At 20 kb the crystallization is dominated by pyrope-rich garnet and very aluminous clinopyroxene (17.5% Al_2O_3). The density of this assemblage (3.5 g/cm^3) is too large to be consistent with the lunar mean density; hence 14310 cannot be the lunar bulk composition.

The orthopyroxene cores to pigeonite in rock 14310 contain a few percent Al_2O_3 and induced Ridley et. al. (1971) to suggest they might be xenocrysts from depth. Reference to Figure 6 demonstrates that our experimental orthopyroxenes grown from melted 14310 in evacuated silica tubes are quite as aluminous as the natural ones. We feel the xenocrypt hypothesis of Ridley et. al. is unnecessary.

The low pressure crystallization of comprehensive fines sample 14259,85 is similar to that of 14310, since both compositions are colinear with that of anorthite. The smaller amount of anorthite in 14259 results in a lower liquidus temperature, 1250°C. Furthermore, the stability field of olivine is enlarged in 14259; a result, we believe, of a difference in oxidation state. With increasing pressure increasingly aluminous orthopyroxene becomes the liquidus phase. At 20 kb pyrope-rich garnet and aluminous clinopyroxene are again the principal crystalline products. The same argument used on 14310 excludes 14259 as the lunar bulk composition.

In rock 14072 the low pressure liquidus phase is olivine (Fo_{85}) appearing at 1275°C, followed by chrome spinel at 1200°C. Pigeonite and plagioclase appear simultaneously at 1180°C. Olivine is consumed with falling temperature, and at pressures above 10 kb it is replaced as the liquidus phase by aluminous orthopyroxene. The occurrence of early pigeonite rather than orthopyroxene in this rock is consistent with an Fe/Fe+Mg ratio greater than that of 14310 and 14259.

Low pressure crystallization of a synthetic glass prepared to study average Apollo 11 anorthositic gabbro (Wood, et. al., 1970) showed an anorthite liquidus at 1485°C with a clear spinel joining at 1450°C. At about 1250°C olivine appears at the expense of the spinel and final crystallization yields plagioclase, olivine and pyroxene with no spinel remaining. The solidus is near 1200°C.

INTERPRETATION OF RESULTS

Figure 5 displays these low pressure results as a function of the bulk Fe/(Fe+Mg) ratio of the compositions. It is interesting that these materials all show liquid saturated with olivine, anorthite, and low calcium pyroxene at temperatures near 1200°C. There is a tendency for the temperature of triple saturation to fall with increasing Fe/(Fe+Mg). This behavior of these samples may be understood in terms of the synthetic system anorthite-silica-forsterite-fayalite (Andersen, 1915; Roeder and Osborn, 1966) (Figure 7). Figure 8 is a projection of the boundary curves in this tetrahedron onto a plane perpendicular to the forsterite-fayalite join. It appears quite similar to Andersen's iron-free end member system but the distortions are caused by plotting molar units and by choosing a section where Fe/(Fe-Mg) is about .3 - .4. The intersection of the silica, pyroxene, and anorthite primary phase fields lies inside the silica-pyroxene-anorthite compositional triangle and hence is a eutectic. The intersection of the olivine, pyroxene, and anorthite primary phase fields lies outside the olivine-pyroxene-anorthite compositional triangle and hence

is a peritectic. Bulk compositions within the olivine-pyroxene-anorthite triangle complete equilibrium crystallization on this peritectic and produce their first liquids upon partial melting on this peritectic. Our crystallization experiments show that this point must be at about 1200°C in samples of Fe/(Fe+Mg) $\stackrel{\sim}{=}$ .3 - .4 and at lower temperatures for higher values of Fe/(Fe+Mg).

It can easily be seen that 14310 and 14259 fall into the plagioclase primary phase field while 14072 falls in the olivine field. It should be noted that the path away from anorthite through 14310 and 14259 projects very close to the peritectic, explaining the simultaneous appearance of olivine and pyroxene and subsequent disappearance of olivine. On the other hand the path through 14072 from olivine also projects near the peritectic, explaining the simultaneous appearance of pyroxene and plagioclase in the crystallization of 14072. The olivine is not immediately consumed with falling temperature because the bulk composition of 14072 lies within the olivine-pyroxene-anorthite triangle. The slightly lower temperature of the peritectic in 14072 and the appearance of a pigeonitic low calcium pyroxene rather than orthopyroxene is a result of the higher Fe/(Fe+Mg)

of 14072. Figures 9 and 10 are projections within the tetrahedron which show the Fe/(Fe+Mg) variable. These figures and Figure 8 have plotted on them the compositions of residual glasses produced in our crystallization experiments from which the boundary curves were determined. Figure 10 demonstrates the shift in Fe(Fe+Mg) caused by the oxidation effects discussed below.

Oxidation state of 14310

El Goresy et. al. (1971, 1972) have noted the assemblages ulvöspinel-ilmenite-iron metal and fayalite-silica-iron metal in 14310 and other Apollo 14 igneous rocks and made an argument for extreme subsolidus reduction. We have also observed these features and concur with their interpretation as the most rational explanation of the following observations. While our experimental crystallization sequence matches that deduced from textural study of 14310 and 14072, our experimental pyroxenes and olivines are considerably more magnesian than the natural ones (Figure 6). This suggests that the reduction of the iron, which effectively lowers the FeO content of the silicate liquid from which the ferromagnesian phases crystallize, occurred after those phases had crystallized in the real rock.

As a corollary to these conclusions and the controlled f_{O_2} experiments performed at Edinburgh (Ford et. al., 1972) we may rather closely estimate the f_{O_2} at which 14310 actually crystallized. Ford et. al. performed their experiments at $P_{O_2} = 10^{-12}$ atm and failed to produce either iron droplets or the correct sequence of phases crystallizing (orthopyroxene was missing and spinel appeared as an early phase). The true P_{O_2} of crystallization of 14310 is therefore below 10^{-12} atm. By 10^{-14} atm (M. J. O'Hara, personal communication) orthopyroxene has returned to the crystallization sequence but so have abundant iron droplets which would deplete the liquid in FeO and cause precipitation of pyroxenes more magnesian than the real ones. We may thus say that 14310 crystallized at a P_{O_2} between 10^{-14} and 10^{-12} but was later subjected to a significant reduction.

As an interesting sidelight we point out that the longer interval of olivine crystallization in 14259 (which is colinear with 14310 and anorthite) is probably an oxidation effect. If 14259 composition has not had its iron so strongly reduced or if it was reoxidized as suggested by Griscom and Marquardt (1972) olivine would have an enhanced crystallization interval according to the Ford et. al. experiments.

DISCUSSION OF RESULTS

Near-surface crystallization

The two igneous rock samples we studied, 14310 and 14072, have texturally determined crystallization sequences (Longhi, Walker and Hays, 1972) which are duplicated in our crystallization experiments in evacuated silica tubes. Considering the vessicular nature of both rocks it is evident that the mineralogy and texture of these two rocks were produced by low pressure crystallization. We shall now try to determine what processes were responsible for the compositions of these rocks.

Significance of major element chemistry

Let us consider the low pressure regime. Figure 8 is the appropriate low pressure liquidus diagram as discussed above. Once again note the central role of the olivine-pyroxene-anorthite peritectic and the positions of 14310, 14259, and 14072 relative to this triple saturation point. As noted before, these compositions very nearly fall on the lines joining the peritectic to the liquidus phases of each rock. Can this be an accident? If 14310 were a primary magma as the Apollo Soil Survey (1971) first

proposed, then this would be coincidental.

Plotted also on Figure 8 are the average analyses of preferred glass compositions (B, C, D, and E) found by the Apollo 14 Soil Survey. The abundance weighted average of these glasses is quite close to comprehensive fines 14259. The abundance pattern in which 14310 is so poorly represented is further evidence that 14310 is not a primary composition. By the same logic then some composition near 14259 or B would be expected to be a primary material at the Apollo 14 site. We note with interest that these expected primary compositions are in striking proximity to the peritectic. We also note that glasses B, C, and D are easily interpreted as being controlled by the pyroxene-plagioclase saturation curve emanating from the peritectic. Ford et. al. (1972) have shown experimentally that glass B is indeed doubly saturated with respect to olivine and plagioclase. The observation that 14259 lies slightly within the plagioclase primary phase field is a natural consequence of contamination of a near peritectic composition with a small amount of glass type E, the possible significance of which we will discuss below.

What then is the explanation of the compositions of 14310 and 14072 which are not close to this peritectic? Considering the positions of 14310 and 14072 relative to this peritectic noted above, it is not difficult to imagine that if plagioclase were added to a peritectic liquid, 14310 would result; and if olivine were added to the peritectic, then 14072 would result.

We have concluded that it appears likely that the peritectic composition is important at the Apollo 14 site, but can we argue that feldspar or olivine enrichment in this liquid took place? We have described elsewhere (Longhi, Walker and Hays, 1972) the texturally anomalous large feldspars in 14310 and their compositional pecularities with respect to Fe/Mg ratio. Brown and Peckett (1972) have also noted these large anorthite grains and termed the rock "feldspar-phyric." The percentage of these phenocrysts is difficult to estimate because of a lack of a clear cut-off separating them from the largest lath shaped crystals which are not so clearly phenocrystic. Kushiro (1972) has suggested that there is not enough phenocrystic anorthite to displace 14310 sufficiently from the peritectic composition ($\sim$ 15% phenocrysts necessary). However, photos of 30 thin

sections of 14310 reveal that it is quite heterogeneous with respect to phenocryst abundance and that 15% phenocrysts is well within the observed range. We feel that the colinear nature of peritectic - 14310 - anorthite and the textural and compositional peculiarities of the feldspar phenocrysts support the feldspar addition hypothesis. In 14072 we have noted the conspicuous olivine phenocrysts and the resorbed nature of the olivine in thin section (Longhi, Walker and Hays, 1972).

We feel the textural and chemical evidence of the rocks supports the hypothesis that olivine and plagioclase have been introduced into "proto" 14072 and 14310 liquids respectively. In our experimental charges plagioclase remains suspended in 14310 liquid and olivine very quickly sinks in 14072 liquid. Floatation or concentration by eddy currents of plagioclase in a body of peritectic magma with complementary sinking of olivine is a convenient mechanism for producing the desired phenocrystic rocks. The slightly higher Fe/(Fe+Mg) of 14072 may be explained as a natural consequence of its being lower in the magma body where equilibrium fractional crystallization with olivine can lead to iron enrichment. 14072 must be low in this body to receive sinking crystals.

We do not necessarily believe that 14072 and 14310 were produced in the very same magma chamber although the ages of the two are the same by Rb-Sr and Ar^{39}-Ar^{40} (Compston et. al., 1972; York et. al., 1972). Helmke and Haskin (1972) have determined that the REE of 14072 although enriched, do not show the spectacular concentrations of 14310 making it unlikely that 14310 and 14072 are actually comagmatic.

Figure 8 plots the composition of "howarditic" green glass (H) identified by Marvin et. al . (1972) in various lunar soils. It is quite close to 14072 in composition and we feel that shock melting of material like 14072 is more likely than the survival of primitive nebular materials as an origin for this glass.

Origin of triply-saturated liquids

It appears that olivine-pyroxene-anorthite peritectic liquid can explain many features of Apollo 14 rock and soil chemistry. From the soil glass abundance data and the indirect arguments from 14310 and 14072 we would expect a good deal of it to have been produced at some time. How was it produced? One property of a peritectic as opposed to a eutectic is that it is difficult to generate large

amounts of peritectic liquid in any crystallization process. During equilibrium crystallization, a liquid composition which reaches the peritectic from some higher temperature either concludes its crystallization there or pauses for reaction of olivine and liquid and then continues to change composition. During fractional crystallization, a liquid which reaches the peritectic has no tendency to remain there as it loses heat but keeps changing in composition. In such a situation the only way to get a substantial quantity of peritectic liquid is to extract that liquid from some larger body of liquid which has just reached this delicate chemical and thermal balance. For this reason Wood et. al. (1971) and Wood's (1972) norite layer (essentially this peritectic in composition) within the moon is highly improbable. First, to segregate this much peritectic liquid while cooling the moon would be difficult and then to keep it from differentiating given the tendency of olivine to sink and requiring plagioclase to float to form anorthosite is hard to accomplish.

Partial melting of the lunar crust

Fortunately a peritectic is not a "no-way" street.

Upon adding heat to an olivine-pyroxene-plagioclase assemblage, any amount of peritectic liquid can be generated until one of the phases pyroxene or plagioclase is exhausted. Peritectic liquid is the partial melting product of any bulk composition in the olivine-pyroxene-plagioclase volume. Partial melting of an olivine-low calcium pyroxene-plagioclase assemblage seems the most reasonable mechanism for producing the primary material of the Apollo 14 landing site. Although the source material could be of any composition within the olivine-pyroxene-anorthite volume, there is one lunar rock type which is a particularly attractive candidate. In Figures 8, 9, and 10, glass E of the soil survey and the anorthositic gabbro of Wood et. al.(1970) fall close together in the olivine-pyroxene-anorthite volume. Furthermore this composition is reminiscent of the Surveyor 7 analysis of Tycho ejecta (Patterson, et. al, 1969). Reid et. al.(1972) have recently furnished a preprint noting the remarkable uniformity and distribution of this component around the moon. The collective conclusion is that this anorthositic gabbro is representative of the lunar highlands. Note that the solidus is in the neighborhood of 1200°C in our

synthetic anorthositic gabbro. It is plausible that partial melting of this highland material and subsequent differentiation of that liquid would produce the materials sampled by Apollo 14. If such is the case the highlands mineralogically should be olivine, low calcium pyroxene, and plagioclase. 14310 has orthopyroxene and nearly simultaneously pigeonite while 14072 has pigeonite. It is possible that both varieties of low calcium pyroxene may be in the highlands as a consequence (or cause?) of the Fe/(Fe+Mg) of the peritectic liquid.

When did this melting take place? Ganapathy et. al., (1972) and others have suggested that 14310 is melted soil on the basis of trace element data. Others have suggested this conclusion on the basis of the superficial major element similarity of fines 14259 and rock 14310. The Imbrian impact event is commonly supposed to be the excavation which sprinkled the Fra Mauro formation about the lunar surface and could provide the necessary energy. Two lines of evidence suggest that the Imbrian event is not the immediate cause of the 14310 melting. Ridley et. al., (1972) noted many rock types like 14310 incorporated as clasts in the Fra Mauro breccias which implies pre-Imbrian generation.

Papanastassiou and Wasserburg (1971) find evidence for a pre-Imbrian crystallization date in the Rb/Sr systematics for 14310. This is not to say that a pre-Imbrian impact might not have produced the earlier heat input which caused the partial melting. This seems a very likely mechanism for incorporating the trace elements characteristic of a meteorite contaminated soil. The alternate possibility is that some internal heating anomaly produced high level partial melts prior to the Imbrian event.

Origin of KREEP

Hubbard and Gast (1972) have shown that 14310 has a trace element enrichment like the KREEP component first recognized at the Apollo 12 site. The peritectic composition and its differentiates are strongly reminiscent of KREEP. Meyer (1972) has shown that Apollo 15 KREEP is mineralogically quite like the Apollo 14 Fra Mauro basalts. Taylor et. al., (1971) have shown that the Apollo 14 soil is heavily dominated by this KREEP material. The enormous enrichments in REE (200-300 x chondrites) but the compositionally primitive Fe/Mg ratio clearly favor a small degree of partial

melting rather than extensive fractional crystallization to produce the Fra Mauro type KREEP basalts of which 14310 is an example. The two stage process of enrichment implicit in melting a lunar crust which itself is a differentiate of some more primitive lunar material is ideally suited to producing these enrichments.

Partial melting of lunar interior?

One possible alternative explanation is that these two rocks are partial melts of the lunar interior which have suffered only minor modification in transit to the lunar surface where they crystallized. If such is the case rock 14310 is likely to be derived from a source region or orthopyroxene, clinopyroxene, and spinel as implied by the liquidus assemblages in the pressure interval 12-18 kb corresponding to 240 or 360 km depth. Depths greater than this would imply a garnet-clinopyroxene residue of density too great (>3.5/cc) for the lunar interior on grounds of mean density and moment of inertia of the moon. Derivation at shallower levels by partial melting implies a plagioclase rich source region not too different from the rock itself and is only a degenerate possibility. If 14072 is a partial melt it is most readily derived from the 10 kb (200 km) region

where an olivine-orthopyroxene source region is implied by the liquidus assemblage. Recent work on a synthetic glass of similar composition also shows pigeonite near the liquidus. These implied lunar interiors are not greatly different from the model proposed by Ringwood and Essene (1970) on the basis of their Apollo 11 work. We do not consider partial melting at depth to be a preferred mechanism for generating these lavas when the alternatives above are considered.

Effect of alkali loss

Following Brown and Peckett (1971), Kushiro (1972) has added 3.2% and 1% K to 14310 and finds cotectic behavior of 14310 at 3 kb with respect to olivine, plagioclase, spinel and orthopyroxene. He suggests direct melting of this assemblage at depth as a possible source of 14310 with restored alkalies.

We have performed experiments adding alkalies to 14310 in vacuum. Addition of .4% Na_2O (as $NaHCO_3$) causes orthopyroxene to disappear and greatly increases the amount of olivine at 1200°C. Addition of 2% Na_2O reduced the liquidus temperature below 1250°C so it appears that the large plagioclase crystallization interval is reduced, perhaps

approaching cotectic behavior. Addition of ~1.5% Na_2O allowed plagioclase of composition An 86 to grow presumably near the liquidus at 1250°C. An 86 is more sodic than the phenocrystic plagioclase cores in 14310. Addition of still more Na_2O would certainly make the plagioclase too sodic to be consistent with the natural cores. We feel that Brown and Peckett's estimate of alkali loss must be exaggerated since restoration of that much sodium produces plagioclase too sodic compared to the natural examples. While 14310 may have lost much of the sodium associated with the very late interstitial liquids, its bulk sodium has not been so drastically reduced. We therefore feel that these experiments by Kushiro are not relevant.

SUMMARY AND CONCLUSIONS

Evidence is accumulating that the moon has a differentiated crust some 50 to 100 kilometers in thickness (Toksöz et. al., 1972; Langseth et. al., 1972; Gast and McConnell, 1972; Wood, 1972.) Density, compressional wave velocity, heat production, and major and trace element chemistry of the non-mare portion of this crust seem to be consistent with the hypothesis that a significant portion of the crust consists of anorthositic gabbro.

We have shown here that partial melting of anorthositic gabbro (or indeed of any mixture of the minerals plagioclase-olivine-low calcium pyroxene) will tend to produce significant quantities of liquid having major element chemistry resembling certain Apollo 14 materials. Furthermore, well understood processes of crystal-liquid fractionation acting on such a liquid and its crystalline parents and/or products are capable of explaining in detail the major element chemistry of Apollo 14 crystalline rock samples 14310 and 14072, and of the preferred glass compositions in the Apollo 14 soil including so-called granitic or rhyolitic material. It seems likely to us that such partial melting

events, whether generated by internal or external heat sources, were not uncommon in the early history of the moon, and that much of the material variously described as norite, feldspathic basalts, non-mare basalts, gray mottled fragments, and KREEP, has such an origin.

It also seems likely to us that the trace element and isotopic chemistry of these materials can be accounted for by such a process involving partial melting of pre-enriched crustal materials, but such models remain to be worked out in detail.

ACKNOWLEDGMENTS

We thank D. Chipman, P. Lyttle, C. B. Ma, and M. Campot for assistance with various aspects of the experimental work; D. Weill, J. A. Wood, G. J. Taylor, J. Reid, U. Marvin, and J. L. Warner for their criticism and helpful discussions; and J. A. Wood, M. J. O'Hara, I. Kushiro, A. E. Ringwood, N. Toksöz, R. Williams and the Apollo Soil Survey for making their results available to us in advance of publication. A. Muan arranged an exchange of starting materials, and J. L. Warner provided us with photographs of thirty thin-sections of rock 14310.

This work has been supported by the Committee on Experimental Geology and Geophysics, Harvard University, and by the NASA under grants NGR 22-007-175 and NGR 22-007-199. David Walker is an NSF predoctoral fellow.

REFERENCES

Andersen O. (1915) The system anorthite-forsterite-silica. Amer. Jour. Sci., 4th ser. 39, 407-454.

Apollo Soil Survey (1971) Apollo 14: Nature and origin of rock types in soil from the Fra Mauro formation. Earth Planet. Sci. Lett. 12, 49-54.

Biggar G.M. (1970) Molybdenum as a container for melts containing iron oxide. Ceramic Bulletin 49, 286-288.

Biggar G.M., O'Hara M.J., Peckett A., and Humphries D.J. (1971) Lunar lavas and the achondrites: petrogenesis of protohypersthene basalts and the maria lava lakes. Proc. Second Lunar Sci. Conf., Geochim. Cosmochim. Acta Suppl. 2, Vol. 1, pp. 617-643, MIT Press.

Boyd F.R. and England J. L. (1960) Apparatus for phase equilibrium measurements at pressures up to 50 kilobars and temperatures up to 1750°C. J. Geophys. Res. 65, 741-748.

Boyd F.R. and England J.L. (1963) Effect of pressure on the melting point of diopside, $CaMgSi_2O_6$ and albite, $NaAlSi_3O_8$ in the range up to 50 kilobars. J. Geophys. Res. 68, 311-323.

Brown G.M. and Peckett A. (1971) Selective volatilization on the lunar surface: evidence from Apollo 14 feldspar-phyric basalts. Nature 234, 262-266.

Compston W., Vernon M.J., Berry H., Rudowski R., Gray C.M., and Ware N. (1972) Age and petrogenesis of Apollo 14 basalts (abstract). In Lunar Science - III (editor C. Watkins), pp. 151-153, Lunar Science Institute Contr. No. 88.

El Goresy A., Ramdohr P., and Taylor L.A. (1971) The opaque mineralogy of Apollo 14 crystalline rock 14310 (abstract). In Abstracts With Programs, 1971 Annual Meetings, Geological Society of America, p. 555.

El Goresy A., Ramdohr P., and Taylor L.A. (1972) Fra Mauro crystalline rocks: petrology, geochemistry, and subsolidus reduction of the opaque minerals (abstract). In Lunar Science - III (editor C. Watkins, pp. 224-226, Lunar Science Institute Contr. No. 88.

Ford C.E., Humphries D.J., Wilson G., Dixon D., Biggar G.M., and O'Hara M.J. (1972) Experimental petrology of high-alumina basalt, 14310, and related compositions (abstract). In Lunar Science - III (editor C. Watkins), pp.274-276, Lunar Science Institute Contr. No. 88.

Ganapathy R., Laul J.C., Morgan J.W., and Anders E. (1972) Moon: possible nature of the body that produced the Imbrian basin, from the composition of Apollo 14 samples. Science 175, 55-58.

Gast P.W. and McConnell R.K. Jr., (1972) Evidence for initial chemical layering of the moon (abstract). In Lunar Science - III (editor C. Watkins), pp. 289-290, Lunar Science Institute Contr. No. 88.

Griscom D.L. and Marquardt C.L. (1972) Electron spin resonance studies of iron phases in lunar glasses and simulated lunar glasses (abstract). In Lunar Science - III (editor C. Watkins), pp. 341-343, Lunar Science Institute Contr. No. 88.

Helmke P.A. and Haskin L.A. (1972) Rare earth and other trace elements in Apollo 14 lunar samples (abstract) In Lunar Science - III (editor C. Watkins), pp. 366-368, Lunar Science Institute Contr. No. 88.

Hubbard N.J. and Gast P.W. (1972) Chemical composition of Apollo 14 materials and evidence for alkali volatilization (abstract). In Lunar Science - III (editor C. Watkins), pp. 407-409, Lunar Science Institute Contr. No. 88.

Johannes W., Bell P.M., Mao H.K., Boettcher A.L., Chipman D.W., Hays J.F., Newton R.C., and Seifert F. (1971) An interlaboratory comparison of piston-cylinder pressure calibration using the albite-breakdown reaction. Contrib. Mineral. Petrol. 32, 24-38.

Kushiro I. (1972) Petrology of high-alumina basalt (abstract). In Lunar Science - III (editor C. Watkins), pp. 466-468, Lunar Science Institute Contr. No. 88.

Langseth M.G. Jr., Clark S.P. Jr., Chute J. Jr., and Keihm S. (1972) The Apollo 15 lunar heat flow measurement (abstract). In Lunar Science - III (editor C. Watkins), pp. 475-477, Lunar Science Institute Contr. No. 88.

Longhi J.L., Walker D., and Hays J.F. (1972) Petrography and crystallization history of Apollo 14 crystalline rocks. this volume.

Mao H.K., and Bell P.M. (1971) Behavior of thermocouples in the single-stage piston-cylinder apparatus. Carnegie Inst. Wash. Yearbook 69, 207-216.

Marvin U.B., Reid J.B. Jr., Taylor G.J., and Wood J.A. (1972) Lunar mafic green glasses, howardites, and the composition of undifferentiated lunar material (abstract) In Lunar Science - III (editor C. Watkins), pp. 507-509, Lunar Science Institute Contr. 88.

Papanastassiou D.A. and Wasserburg G.J. (1971) Rb-Sr ages of igneous rocks from the Apollo 14 mission and the age of the Fra Mauro formation. Earth Planet. Sci. Lett. 12, 36-48.

Patterson J.H., Franzgrote E.J., Turkevich A.L., Anderson W.A., Economov T.E., Griffin H.E., Grotch S.L., and Sowinski K.P. (1969) Alpha-scattering experiment on Surveyor 7: comparison with Surveyors 5 and 6. J. Geophys. Res. 74, 6120-6148.

Reid A.M., Ridley W.I., Harmon R.S., Warner J., Brett R., Jakeš P., and Brown R.W. (1972) Feldspathic basalts in lunar soils and the nature of the lunar highlands. preprint furnished by the authors.

Ridley W.I., Williams R.J., Takeda H., Brown R.W., and Brett R. (1971) Petrology of Fra Mauro basalt 14310 (abstract). In Abstracts With Programs, 1971 Annual Meetings, Geological Society of America, pp. 682-683.

Ridley W.I., Williams R.J., Brett R., Takeda H., and Brown R.W. (1972) Petrology of lunar basalt 14310 (abstract). In Lunar Science - III (editor C. Watkins), pp. 648-650, Lunar Science Institute Contr. No. 88.

Ringwood A.E. and Essene E. (1970) Petrogenesis of Apollo 11 basalts, internal constitution and origin of the moon. Proc. Apollo 11 Lunar Sci. Conf., Geochim. Cosmochim. Acta Suppl. 1, Vol. 1, pp. 769-799.

Ringwood A.E., Green D.H., and Ware N.G. (1972) Experimental Petrology and Petrogenesis of Apollo 14 basalts (abstract). In Lunar Science - III (editor C. Watkins), pp. 654-656, Lunar Science Institute Contr. No. 88.

Roeder P.L. and Osborn E.F. (1966) Experimental data for the system MgO-FeO-Fe_2O_3-$CaAl_2Si_2O_8$-SiO_2 and their petrologic implications. Amer. Jour. Sci. 264, 428-480.

Taylor S.R., Muir P., and Kaye M. (1971) Trace element chemistry of Apollo 14 lunar soil from Fra Mauro. Geochim. Cosmochim. Acta 35, 975-981.

Toksöz M.N., Press F., Anderson K., Dainty A., Latham G., Ewine M., Dorman J., Lammlein D., Sutton G., Duennebier F., and Nakamura Y. (1972) Velocity structure and properties of the lunar crust (abstract). In Lunar Science - III (editor C. Watkins), pp. 758-760, Lunar Science Institute Contr. No. 88.

Walker D. and Hays J.F. (1972) Diffusion of iron into molybdenum at 10 kilobars. Met. Trans. in press.

Wood J.A., Dickey J.S. Jr., Marvin U.B., and Powell B.N. (1970) Lunar anorthosites. Science 167, 602-604.

Wood J.A., Marvin U.B., Reid J.B. Jr., Taylor G.J., Bower J.F., Powell B.N., and Dickey J.S. Jr. (1971) Mineralogy and petrology of the Apollo 12 lunar sample. Smithsonian Astrophysical Observatory Special Report 333.

Wood J.A. (1972) The nature of the lunar crust and composition of undifferentiated lunar material. submitted to The Moon for publication.

York D., Kenyon W.J., and Doyle R.J. (1972) ^{40}Ar - ^{39}Ar ages of Apollo 14 and 15 samples (abstract). In Lunar Science - III (editor C. Watkins), pp. 822-824, Lunar Science Institute Contr. No. 88.

TABLE 1. RESULTS OF QUENCHING EXPERIMENTS

Results of Experiments on 14310

P(kb)	Run	Starting Material	T°C	Duration (hours)	Capsule	Results
0	71	Powder (1)	1320	21.5	Mo	glass
0	72	Powder (1)	1320	21.5	Fe	glass
0	73	Powder (1)	1320	10.7	Mo	glass
0	79	Powder (2)	1320	11.	Mo	glass
0	80	Powder (2)	1320	9.7	Fe	glass
0	48	Powder (1)	1319	10.8	Fe	glass
0	46	Powder (1)	1319	5.0	Fe	glass + plag
0	21	Powder (1)	1317	10.5	Mo	glass
0	63	Powder (1)	1315	50.8	Pt	glass + spinel + (?) plag
0	38	Glass (3)	1304	46.2	Mo	glass + plag
0	37	Powder (1)	1303	65.	Mo	glass + plag
0	20	Powder (1)	1302	3.8	Mo	glass + plag
0	16	Powder (1)	1277	4.5	Mo	glass + plag
0	28	Powder (1)	1252	21.2	Mo	glass + plag
0	15	Powder (1)	1227	10.7	Mo	glass + plag
0	40	Glass (4)	1204	12.	Mo	glass + plag
0	23	Powder (1)	1202	24.	Mo	glass + plag + opx + ol(trace)
0	68	Powder (1)	1200	21.	Fe	glass + plag + opx + ol
0	69	Powder (2)	1200	111.	Mo	glass + plag + opx + ol
0	67	Powder (5)	1190	14.8	Mo	glass + plag + opx + pig
0	41	Glass (6)	1184	21.8	Mo	glass + plag + pig + opx
0	25	Glass (7)	1177	41.	Mo	glass + plag + pig + opx
0	42	Glass (8)	1164	72.	Mo	glass + plag + pig + (opx)
0	34	Powder (1)	1152	48.	Mo	glass + plag + opx + pig
0	49	Glass (4)	1104	82.5	Mo	glass + plag + (opx) + pig + trid

TABLE 1. RESULTS OF QUENCHING EXPERIMENTS (continued)

Results of Experiments on 14310

P(kb)	Run	Starting Material	T°C	Duration (hours)	Capsule	Results
		* (14310 composition modified)				
0	65	(9)*	1200	47.5	Mo	glass+plag+opx+ol(tr)+sp(tr)
0	66	(9)*	1200	117.0	Mo	glass + plag + opx
0	62	(10)*	1200	48.5	Mo	glass + plag + ol + opx
0	81	(11)*	1200	28.5	Mo	glass + plag + ol
0	82	(12)*	1250	56.	Mo	glass + plag
0	83	(13)*	1250	48.	Mo	glass
5	71	Powder (1)	1325	1.8	Graphite	glass
5	17	Powder (1)	1300	2.	Mo	glass + plag
5	55	Powder (1)	1265	3.3	Mo	glass + plag
5	4	Powder (1)	1250	2.	Mo	glass + plag + pig + opx
5	57	Glass (14)	1200	4.5	Mo	glass + plag
5	7	Powder (1)	1150	12.	Mo	glass + plag + pig + (opx)
10	19	Powder (1)	1325	2.	Mo	glass
10	22	Powder (1)	1310	2.2	Mo	glass + plag
10	6	Powder (1)	1260	2.	Mo	glass + plag + pig + (opx)
15	9	Powder (1)	1350	2.	Mo	glass
15	12	Powder (1)	1340	2.	Mo	glass + spinel
15	53	Powder (1)	1340	3.	Mo	glass + (?) opx
15	31	Powder (1)	1333	4.4	Mo	glass + cpx
15	45	Glass (15)	1330	6.	Mo	glass
15	51	Powder (1)	1326	3.5	Mo	glass
15	36	Powder (1)	1325	6.	Mo	glass
15	54	Powder (1)	1325	5.	Mo	glass + spinel + plag + (?) cpx
15	3	Powder (1)	1325	2.5	Mo	glass + spinel + plag + cpx
15	39	Glass (16)	1315	9.7	Mo	glass

TABLE 1. RESULTS OF QUENCHING EXPERIMENTS (continued)

Results of Experiments on 14310

P(kb)	Run	Starting Material	T°C	Duration (hours)	Capsule	Results
15	35	Powder (1)	1300	5.2	Mo	glass + spinel + (?) px
15	52	Powder (1)	1300	3.5	Mo	glass + sp + cpx+(?)opx + plag
15	13	Powder (1)	1225	13.5	Mo	glass + pig + (?)opx + plag
17.5	26	Powder (1)	1340	6.	Mo	glass + (?) opx
17.5	56	Powder (1)	1340	3.	Mo	glass + spinel
17.5	32	Powder (1)	1250	24.	Mo	glass + garnet + cpx
20	5	Powder (1)	1405	2.	Mo	glass
20	11	Powder (1)	1375	2.	Mo	glass + (?) garnet
20	47	Glass (15)	1365	6.2	Mo	glass
20	27	Powder (1)	1365	3.	Mo	glass + garnet + cpx
20	14	Powder (1)	1350	3.	Mo	glass + garnet + cpx
20	43	Glass (18)	1325	6.	Mo	glass
20	8	Powder (1)	1250	11.5	Mo	glass + garnet + cpx
20	18	Powder (1)	1200	12.5	Mo	glass + garnet + pig+cpx+plag
20	44	Powder (1)	1150	24.	Mo	glass + garnet + px + (?) sp
20	24	Glass (19)	1150	59.	Mo	(?)glass+ garnet + cpx

TABLE 1. RESULTS OF QUENCHING EXPERIMENTS (continued)

Results of Experiments on 14259

P(kb)	Run	Starting Material	T°C	Duration (hours)	Capsule	Results
0	56	Powder (20)	1252	1.5	Mo	glass
0	55	Powder (20)	1242	1.2	Mo	glass + plag
0	58	Powder (20)	1227	5.2	Mo	glass + plag
0	51	Powder (20)	1202	9.7	Mo	glass + plag + olivine
0	57	Powder (20)	1166	8.	Mo	glass+plag+ol+opx+(?)pig
5	16	Powder (20)	1250	2.5	Mo	glass
5	22	Powder (20)	1240	3.	Mo	glass + plag
5	40	Glass (21)	1240	3.	Mo	glass
5	45	Glass (21)	1230	3.	Mo	glass
5	21	Powder (20)	1225	2.	Mo	glass + plag + opx
5	17	Powder (20)	1200	4.	Mo	glass + plag + pig + opx
5	19	Powder (20)	1175	4.	Mo	glass + plag + pig + opx
5	24	Powder (20)	1150	8.	Mo	glass + plag + pig + (?)opx
5	43	Glass (21)	1150	8.	Mo	glass + plag + pig
10	49	Powder (20)	1290	2.	Mo	glass
10	14	Powder (20)	1275	3.	Mo	glass
10	46	Powder (20)	1275	2.	Mo	glass + plag + opx
10	23	Powder (20)	1260	3.	Mo	glass + pig
10	41	Glass (22)	1260	3.	Mo	glass + pig
10	10	Powder (20)	1250	6.5	Mo	glass + plag + pig + (?) opx
10	18	Powder (20)	1225	3.8	Mo	glass + plag + pig
10	25	Powder (20)	1175	6.5	Mo	glass + plag + pig
12.5	52	Powder (20)	1150	24.	Mo	glass + plag + garnet +cpx+opx
15	39	Powder (20)	1360	2.	Mo	glass
15	36	Powder (20)	1350	1.7	Mo	glass
15	42	Powder (20)	1340	3.2	Mo	glass

TABLE 1. RESULTS OF QUENCHING EXPERIMENTS (continued)

Results of Experiments on 14259

P(kb)	Run	Starting Material	T°C	Duration (hours)	Capsule	Results
15	50	Powder (20)	1330	2	Mo	glass + opx
15	47	Glass (23)	1325	3.3	Mo	glass
15	37	Powder (20)	1325	3.2	Mo	glass + garnet + cpx + opx
15	28	Powder (20)	1250	10.	Mo	glass + garnet + cpx
20	35	Powder (20)	1425	2.	Mo	glass
20	38	Powder (20)	1410	2.7	Mo	glass
20	44	Powder (20)	1405	2.7	Mo	glass + garnet + cpx
20	48	Glass (24)	1405	2.3	Mo	glass
20	34	Powder (20)	1400	3.	Mo	glass + garnet + cpx
20	33	Powder (20)	1375	1.5	Mo	glass + garnet + cpx
20	32	Powder (20)	1325	3.	Mo	glass + garnet + cpx
20	11	Powder (20)	1250	12.5	Mo	glass + garnet + cpx
20	27	Powder (20)	1200	12.7	Mo	glass + garnet + cpx

TABLE 1. RESULTS OF QUENCHING EXPERIMENTS (continued)

Results of Experiments on 14072

P(kb)	Run	Starting Material	T°C	Duration (hours)	Capsule	Results
0	19	Powder (25)	1285	24	Mo	glass
0	10	Powder (25)	1262	19.8	Mo	glass + olivine
0	6	Powder (25)	1212	17.5	Mo	glass + olivine
0	12	Powder (25)	1190	24.5	Mo	glass + olivine + spinel
0	20	Glass (26)	1175	54.2	Mo	glass + sp + pig + (aug) + ol
0	18	Powder (25)	1175	48.	Mo	glass + sp + pig + plag + ol
0	26	Powder (25)	1170	148.	Mo	glass + sp + plag + pig + ol
0	29	Powder (27)	1150	44.	Mo	glass + (?)ol + plag + pig + sp
0	21	Glass (28)	1140	48.	Mo	glass + ol + sp +pig+(opx)+aug
0	11	Glass (17)	1112	70.	Mo	glass + sp + pig + plag
5	30	Powder (25)	1325	2.	Graphite	glass
5	8	Powder (25)	1300	3.	Mo	glass
5	2	Powder (25)	1250	3.5	Mo	glass + ol + (?)sp
5	22	Powder (25)	1200	5.5	Mo	glass + ol + sp + pig
10	5	Powder (25)	1350	3.	Mo	glass
10	3	Powder (25)	1300	3.5	Mo	glass + ol + opx + pig
15	7	Powder (25)	1390	3.2	Mo	glass + (quench cpx)
15	4	Powder (25)	1375	3.	Mo	glass + (?) cpx
15	1	Powder (25)	1350	3.	Mo	glass + opx + (?cpx,trid)
15	23	Powder (25)	1150	15.	Mo	plag + ilm + cpx
20	17	Powder (25)	1440	3.	Mo	glass
20	16	Powder (25)	1420	3.2	Mo	glass + opx + (quench cpx)
20	9	Powder (25)	1400	3.2	Mo	glass + opx + (quench cpx)

Footnotes to Table of Results

(1) Rock powder 14310,138

(2) Rock powder 14310,140 (Supplied by A. Muan)

(3) Glass product of Run 21

(4) Glass produced at 1315°C for 9.2 hours from (1)

(5) Glass and plag produced at 1210°C for 4.5 hours from (1)

(6) Glass made in (4), treated like run 40

(7) Glass from fusing (1) under vacuum

(8) Glass made in (4), treated like runs 40 and 41

(9) Glass and ol and sp and plag and opx produced by hydrothermal crystallization of (1) for 3.5 hours at 5 kb in graphite

(10) Rock powder (1) plus 2% olivine (Fo 74)

(11) Rock powder (1) plus 0.34% Na_2O as $NaHCO_3$

(12) Rock powder (1) plus 1.5% Na_2O as $NaHCO_3$

(13) Rock powder (1) plus 2% Na_2O as $NaHCO_3$; held 3 hours at 1320°C

(14) Glass prepared by fusion of (1) at 1325°C for 0.7 hours at 5 kb

(15) Glass prepared by fusion of (1) at 1315°C for 5 hours at 20 kb

(16) Glass prepared by fusion of (1) at 1400°C at 0.5 hours at 15 kb

(17) Glass and olivine prepared by partial fusion of (25) at 1250°C for 1.5 hours

(18) Glass prepared by fusion of (1) at 1400°C for 0.5 hours at 20 kb

(19) Glass prepared by fusion of (1) at 1400°C for 0.2 hours at 20 kb

(20) Comprehensive fines 14259,85.

(21) Glass prepared by fusion of (20) at 1250°C

(22) Glass prepared by fusion of (20) at 1275°C at 10 kb

(23) Glass prepared by fusion of (20) at 1340°C at 15 kb

(24) Glass prepared by fusion of (20) at 1415°C at 20 kb

(25) Rock powder 14072,3

(26) Glass prepared by fusion of (25) at 1285°C for 24 hours

(27) Sintered powder product of (25) at 1125°C for 205 hours .

(28) Glass plus crystals prepared with run 20

FIGURE CAPTIONS

Fig. 1. Electron microprobe analyses of glasses formed by quenching melted rock powder from 14310,138 held above the liquidus temperature in various capsule materials. Other analyses are plotted for comparison.

Fig. 2. Pressure-temperature diagram for 14310,138.

Fig. 3. Pressure-temperature diagram for 14259,85.

Fig. 4. Pressure-temperature diagram for 14072,3.

Fig. 5. Summary of results from low-pressure quenching experiments.

Fig. 6. Electron microprobe analyses of lunar pyroxenes from 14310,30 and synthetic pyroxenes from experiments on 14310,138.

Fig. 7. Liquidus tetrahedron at atmospheric pressure for the system anorthite-forsterite-fayalite-silica at very low oxygen fugacities (ca. 10^{-15}).

Fig. 8. Projection onto the anorthite-forsterite-silica face of equilibria within the tetrahedron of Fig. 7. Projection is parallel to the forsterite-fayalite join. Field boundaries are located by

analyses of multiply saturated liquids in our experimental runs and hence correspond to an Fe/Fe+Mg ratio of .3 to .4. Boundary curves and their intersections in this figure represent surfaces of two-fold saturation and curves of three-fold saturation respectively within the tetrahedron of Fig. 7.

Fig. 9. Projection onto the anorthite-enstatite-ferrosilite plane of equilibria within the tetrahedron of Fig. 7. Projection point is SiO_2 and boundaries are based on analyses of experimental liquids or inferred from Roeder and Osborn (1966).

Fig. 10. Projection onto the forsterite-fayalite-silica face of equilibria involving plagioclase within the tetrahedron of Fig. 7. Projection point is $CaAl_2Si_2O_8$ and field boundaries are inferred from Roeder and Osborn (1966). The offset of our 14310 experimental liquids from the trace of the soil glasses and the bulk analysis of 14310 is believed to be a result of post-crystallization reduction of 14310 (see text).

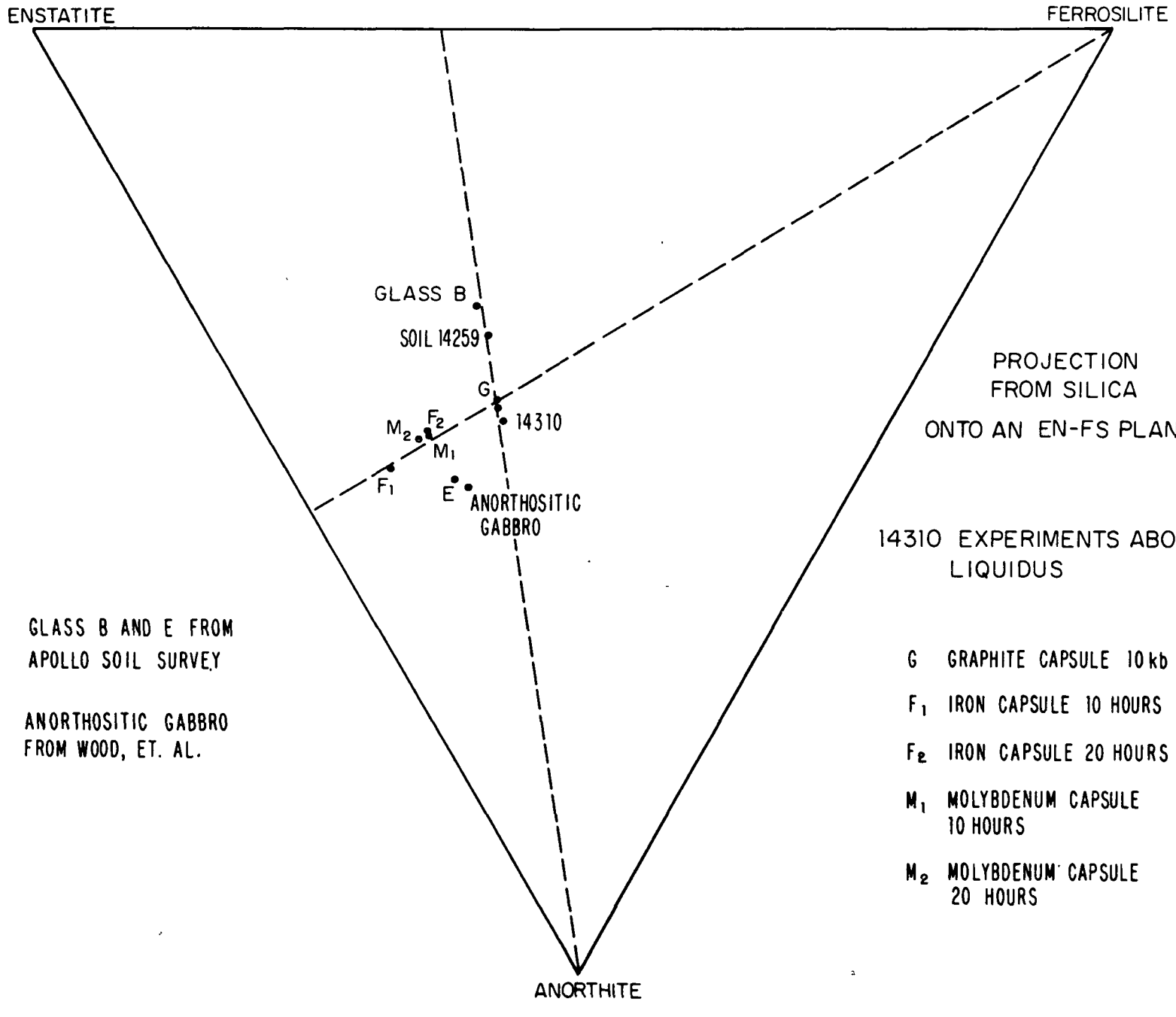
ENSTATITE
FERROSILITE
ANORTHITE
GLASS B
SOIL 14259
G
14310
M_2
F_2
M_1
F_1
E
ANORTHOSITIC GABBRO
PROJECTION FROM SILICA ONTO AN EN-FS PLANE
14310 EXPERIMENTS ABOVE LIQUIDUS
GLASS B AND E FROM APOLLO SOIL SURVEY
ANORTHOSITIC GABBRO FROM WOOD, ET. AL.
G GRAPHITE CAPSULE 10 kb
F_1 IRON CAPSULE 10 HOURS
F_2 IRON CAPSULE 20 HOURS
M_1 MOLYBDENUM CAPSULE 10 HOURS
M_2 MOLYBDENUM CAPSULE 20 HOURS

Fig. 1

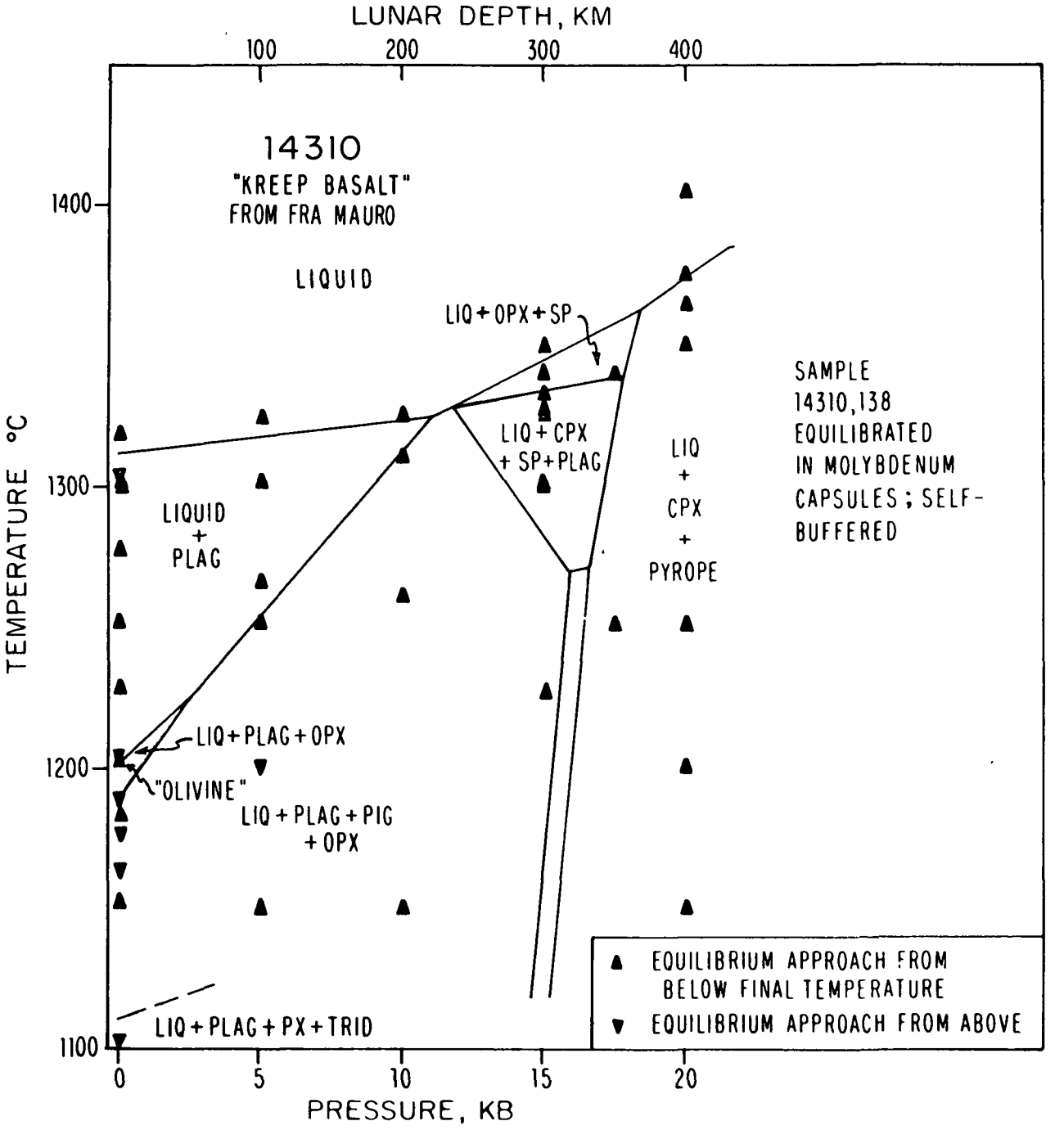
LUNAR DEPTH, KM
100
200
300
400
14310
"KREEP BASALT"
FROM FRA MAURO
LIQUID
LIQ + OPX + SP
LIQ + CPX
+ SP + PLAG
LIQ
+
CPX
+
PYROPE
LIQUID
+
PLAG
LIQ + PLAG + OPX
"OLIVINE"
LIQ + PLAG + PIG
+ OPX
LIQ + PLAG + PX + TRID
SAMPLE
14310,138
EQUILIBRATED
IN MOLYBDENUM
CAPSULES; SELF-
BUFFERED
EQUILIBRIUM APPROACH FROM
BELOW FINAL TEMPERATURE
EQUILIBRIUM APPROACH FROM ABOVE
TEMPERATURE °C
1400
1300
1200
1100
0
5
10
15
20
PRESSURE, KB

Fig. 2

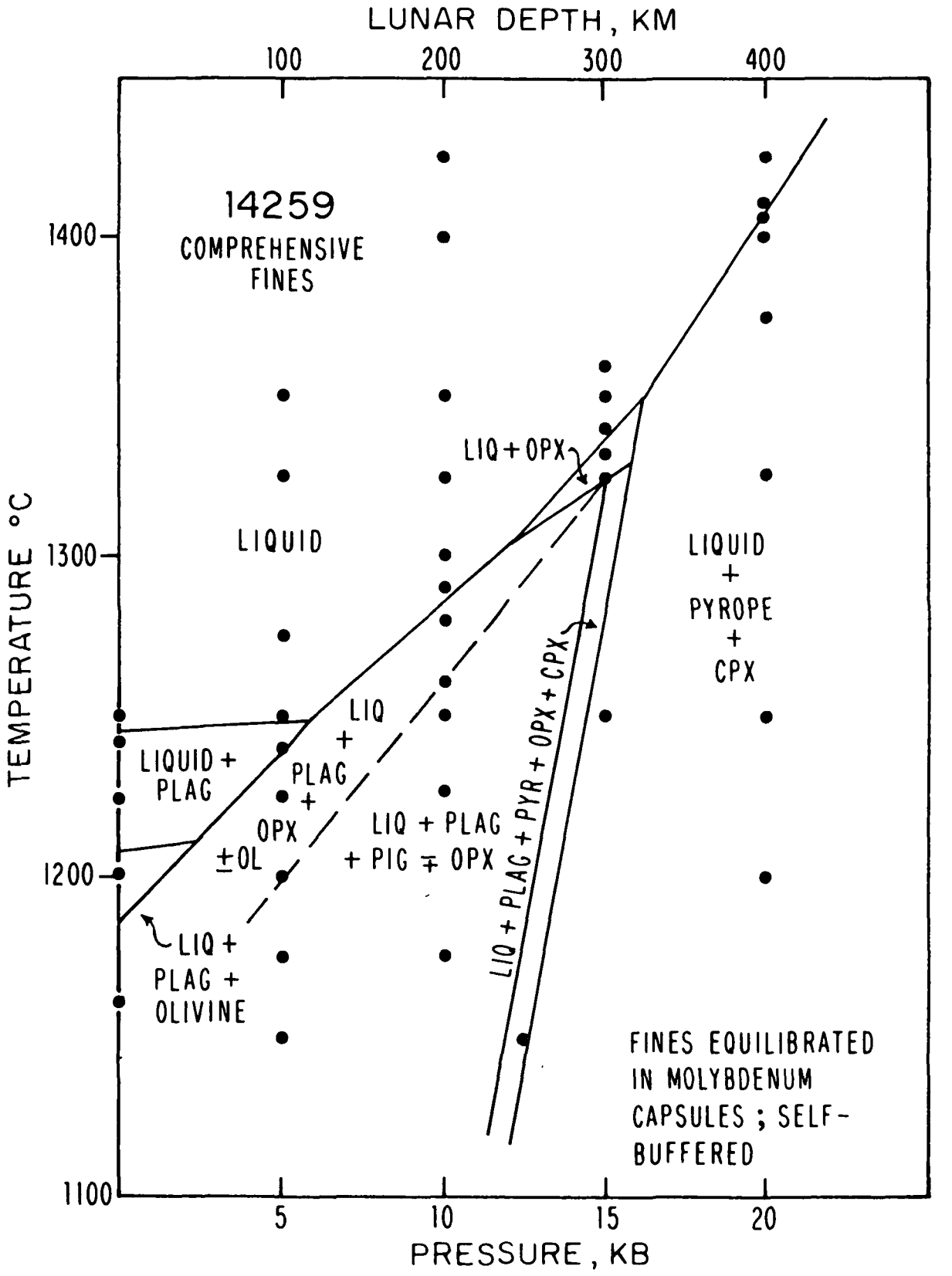
LUNAR DEPTH, KM
100
200
300
400
14259
COMPREHENSIVE
FINES
1400
1300
1200
1100
TEMPERATURE °C
LIQUID
LIQ + OPX
LIQUID
+
PYROPE
+
CPX
LIQ
+
PLAG
+
OPX
±OL
LIQUID +
PLAG
LIQ + PLAG
+ PIG ∓ OPX
LIQ + PLAG + PYR + OPX + CPX
LIQ +
PLAG +
OLIVINE
FINES EQUILIBRATED
IN MOLYBDENUM
CAPSULES ; SELF-
BUFFERED
5
10
15
20
PRESSURE, KB

Fig. 3

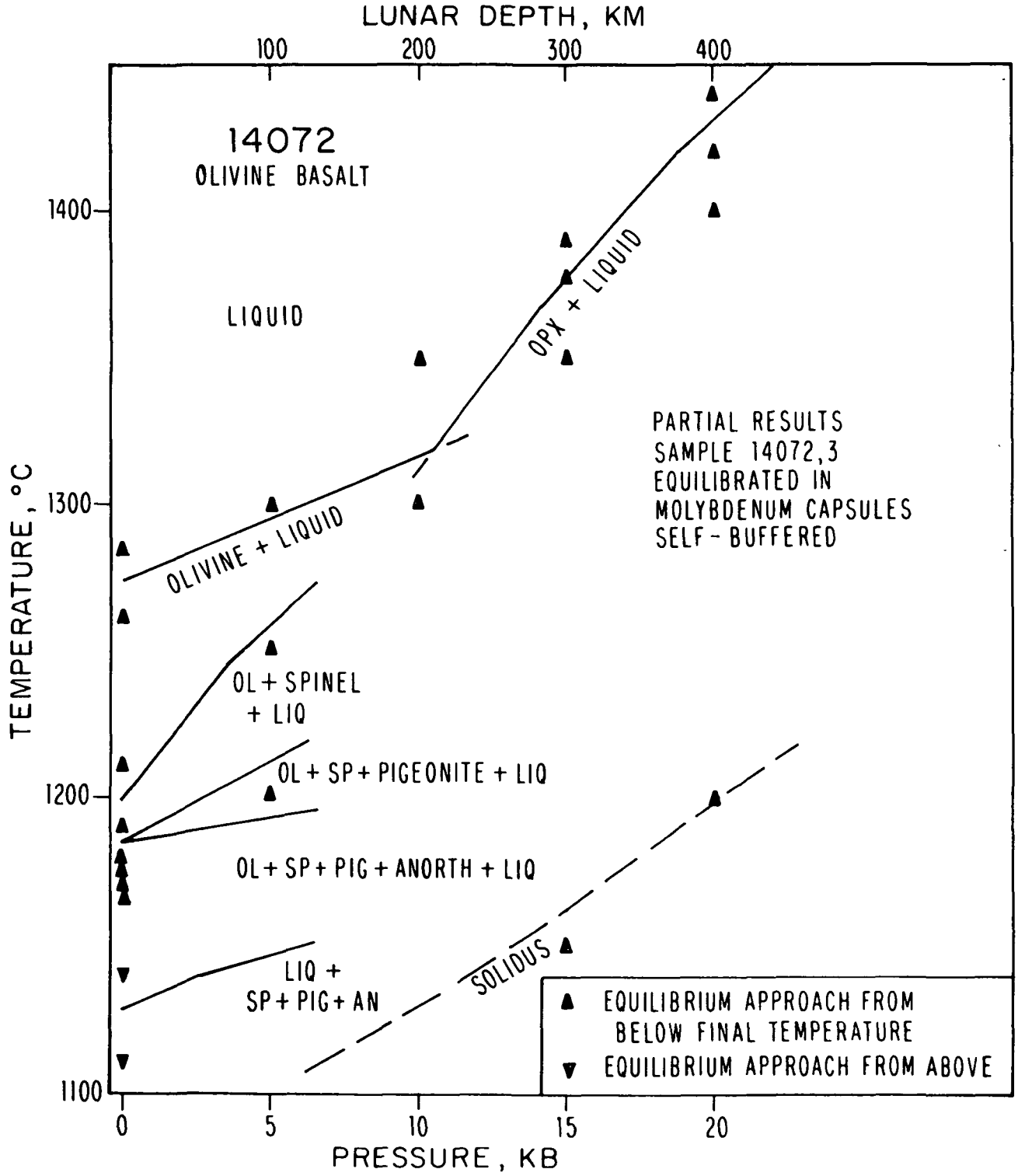
LUNAR DEPTH, KM
100
200
300
400
14072
OLIVINE BASALT
1400
LIQUID
OPX + LIQUID
PARTIAL RESULTS
SAMPLE 14072,3
EQUILIBRATED IN
MOLYBDENUM CAPSULES
SELF - BUFFERED
OLIVINE + LIQUID
1300
OL + SPINEL
+ LIQ
OL + SP + PIGEONITE + LIQ
1200
OL + SP + PIG + ANORTH + LIQ
LIQ +
SP + PIG + AN
SOLIDUS
EQUILIBRIUM APPROACH FROM
BELOW FINAL TEMPERATURE
EQUILIBRIUM APPROACH FROM ABOVE
1100
TEMPERATURE, °C
0
5
10
15
20
PRESSURE, KB

Fig. 4

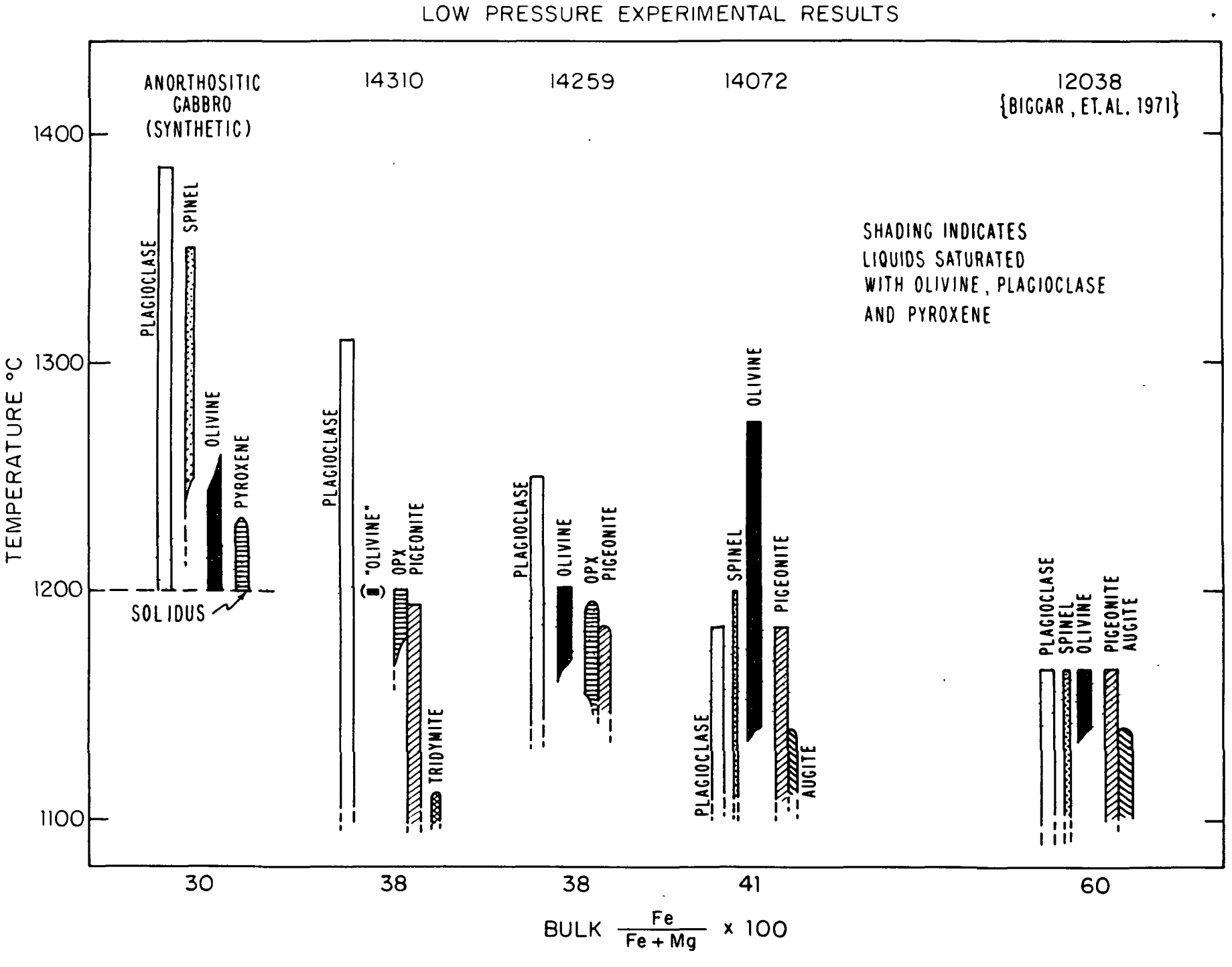
LOW PRESSURE EXPERIMENTAL RESULTS
ANORTHOSITIC GABBRO (SYNTHETIC)
14310
14259
14072
12038 {BIGGAR, ET.AL. 1971}
SHADING INDICATES LIQUIDS SATURATED WITH OLIVINE, PLAGIOCLASE AND PYROXENE
TEMPERATURE °C
1400
1300
1200
1100
PLAGIOCLASE
SPINEL
OLIVINE
PYROXENE
SOLIDUS
"OLIVINE"
OPX
PIGEONITE
TRIDYMITE
AUGITE
30
38
38
41
60
BULK Fe / Fe + Mg x 100

Fig. 5

14310 ORTHOPYROXENES

	NATURAL		EXPERIMENTAL	
SiO_2	51.6	54.5	54.8	54.6
TiO_2	.78	.47	.60	.51
Al_2O_3	3.70	1.26	3.04	2.20
Cr_2O_3	.43	–	.53	.47
FeO	13.8	14.1	5.90	6.98
MgO	27.2	27.2	33.4	33.0
CaO	2.26	1.88	1.54	1.77
K_2O	.09	–	–	–
Na_2O	.03	–	.02	–
SUM	99.9	99.4	99.8	99.5

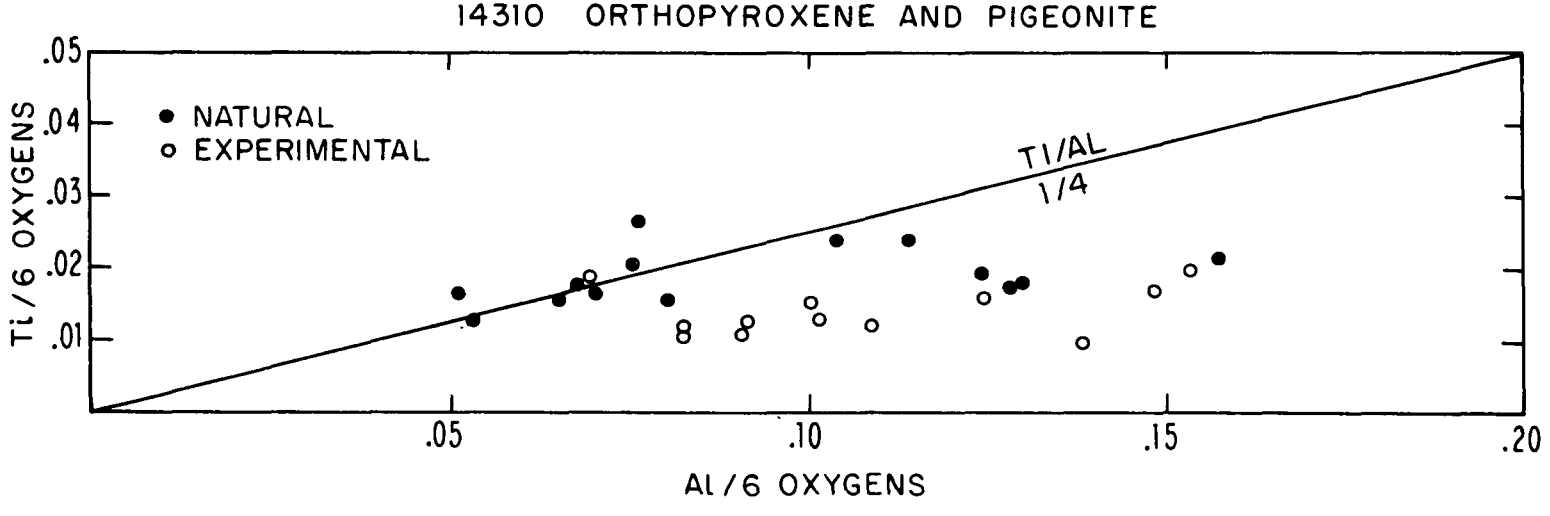

Fig. 6

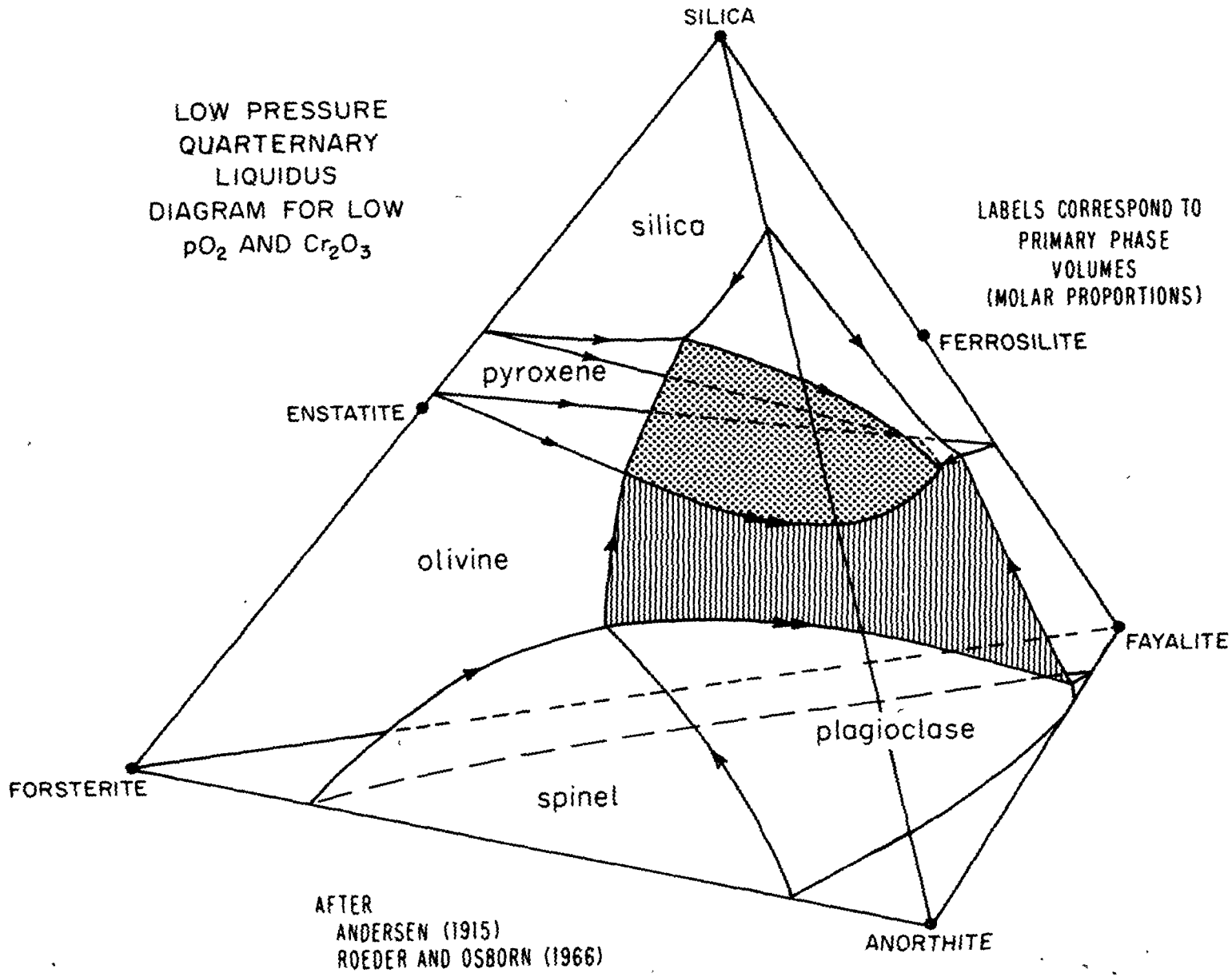
LOW PRESSURE
QUARTERNARY
LIQUIDUS
DIAGRAM FOR LOW
pO_2 AND Cr_2O_3
SILICA
silica
LABELS CORRESPOND TO
PRIMARY PHASE
VOLUMES
(MOLAR PROPORTIONS)
FERROSILITE
pyroxene
ENSTATITE
olivine
FAYALITE
plagioclase
FORSTERITE
spinel
ANORTHITE
AFTER
ANDERSEN (1915)
ROEDER AND OSBORN (1966)

Fig

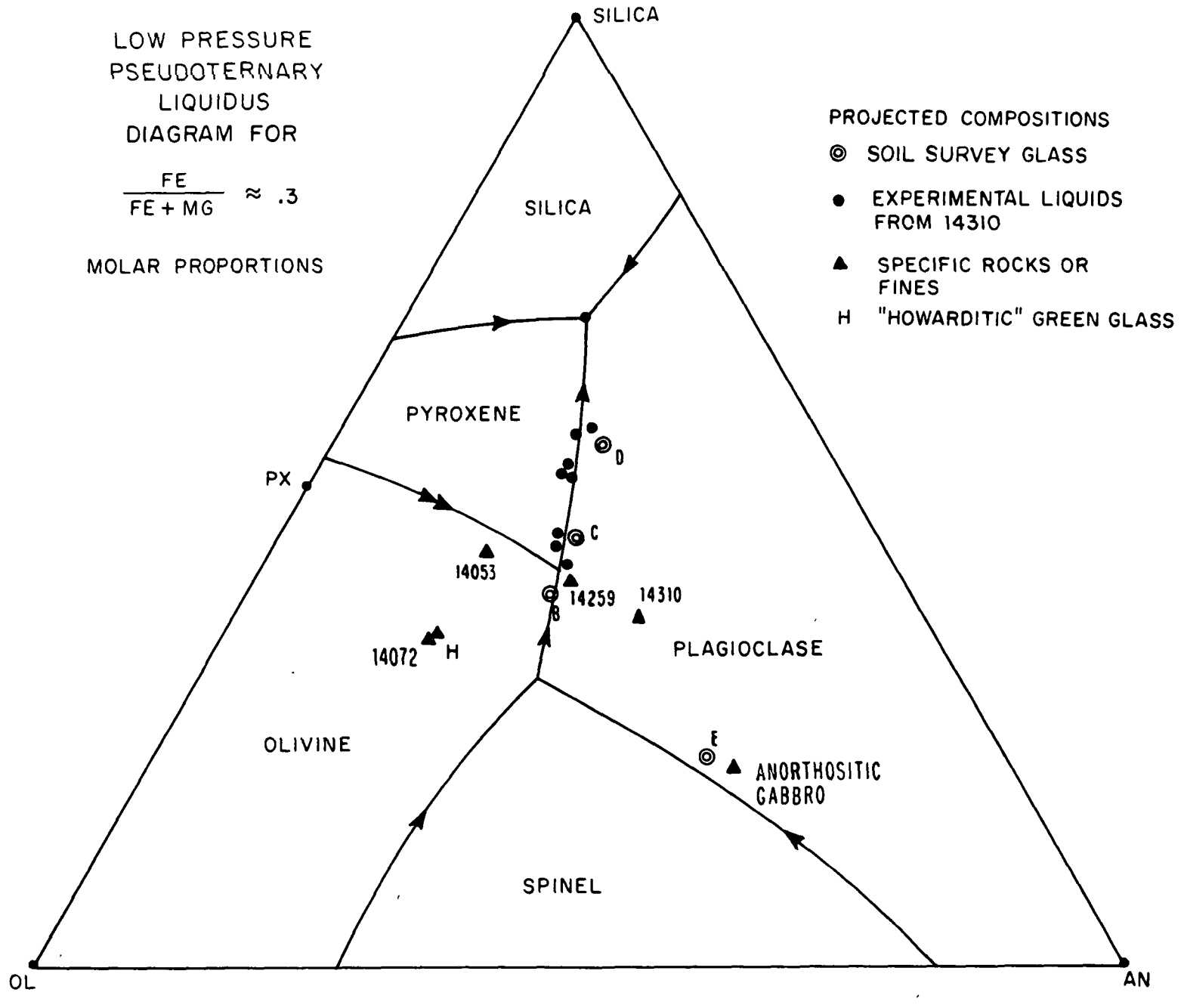
LOW PRESSURE
PSEUDOTERNARY
LIQUIDUS
DIAGRAM FOR
FE / FE + MG ≈ .3
MOLAR PROPORTIONS
SILICA
PROJECTED COMPOSITIONS
SOIL SURVEY GLASS
EXPERIMENTAL LIQUIDS FROM 14310
SPECIFIC ROCKS OR FINES
H "HOWARDITIC" GREEN GLASS
SILICA
PYROXENE
PX
D
C
14053
14259
14310
B
14072
H
PLAGIOCLASE
OLIVINE
E
ANORTHOSITIC GABBRO
SPINEL
OL
AN

Fig. 8

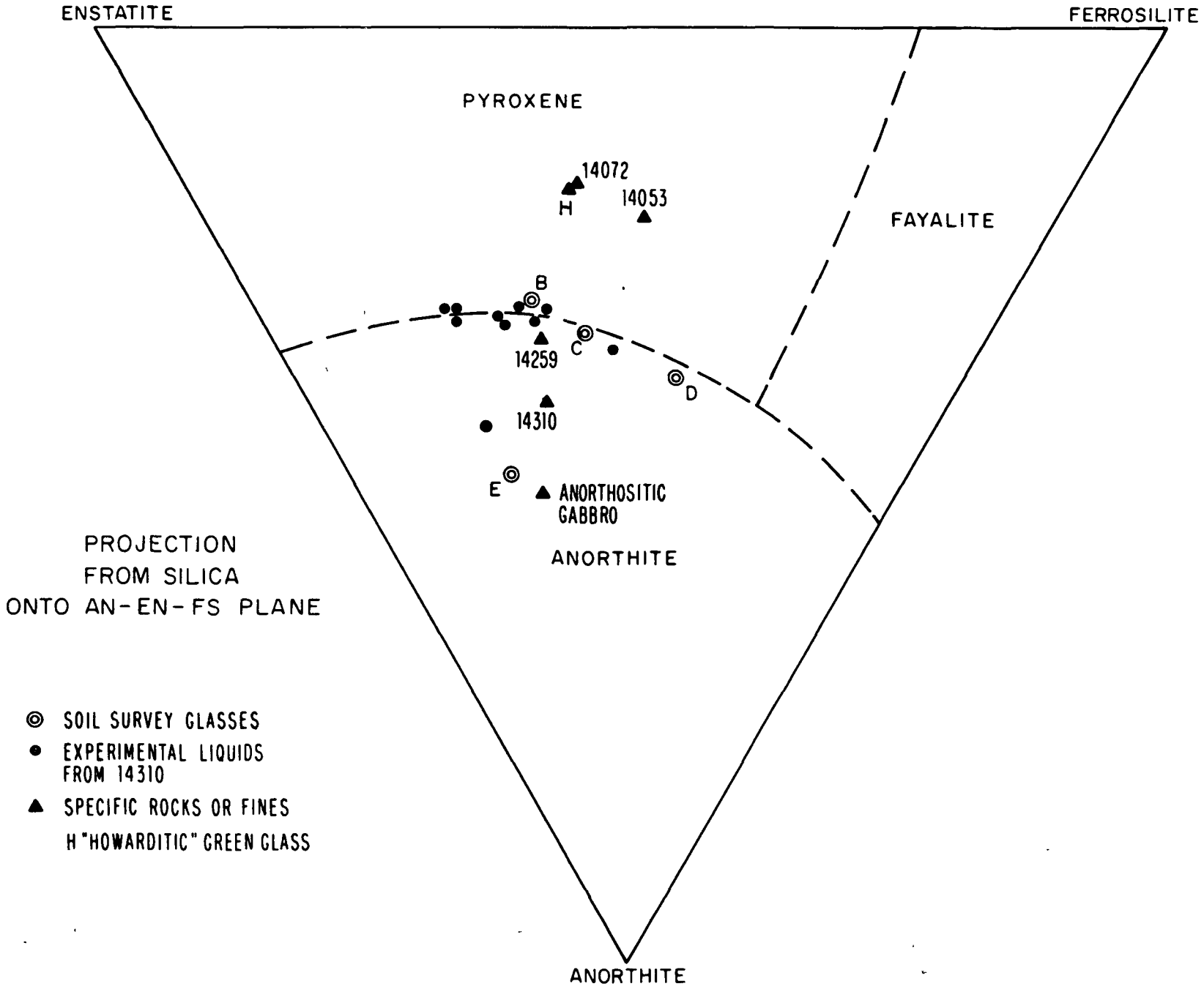
ENSTATITE
FERROSILITE
PYROXENE
14072
H
14053
FAYALITE
B
14259
C
D
14310
E
ANORTHOSITIC GABBRO
ANORTHITE
PROJECTION FROM SILICA ONTO AN-EN-FS PLANE
SOIL SURVEY GLASSES
EXPERIMENTAL LIQUIDS FROM 14310
SPECIFIC ROCKS OR FINES
H "HOWARDITIC" GREEN GLASS
ANORTHITE

Fig. 9

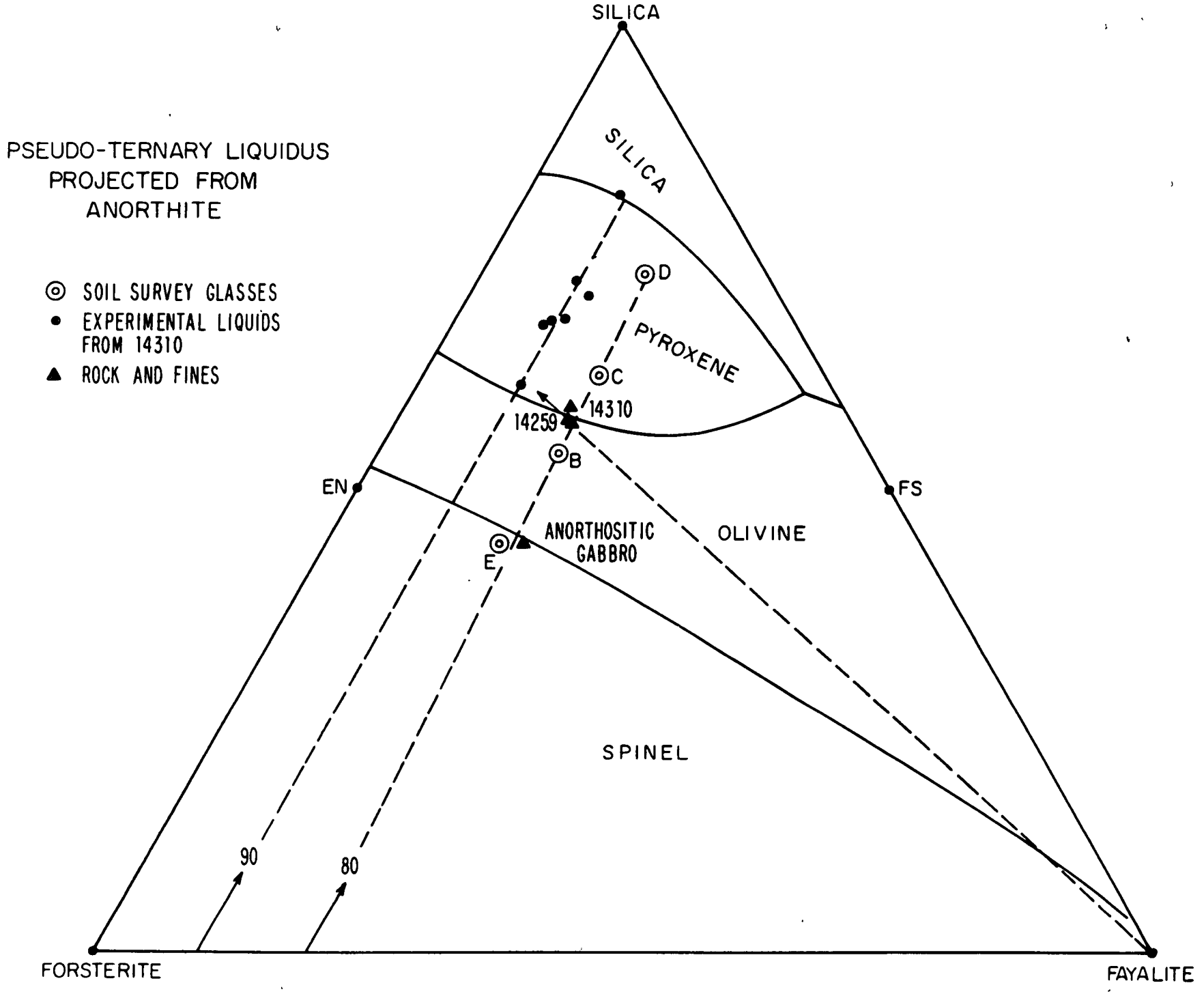
PSEUDO-TERNARY LIQUIDUS
PROJECTED FROM
ANORTHITE
SOIL SURVEY GLASSES
EXPERIMENTAL LIQUIDS
FROM 14310
ROCK AND FINES
SILICA
SILICA
PYROXENE
D
C
B
E
14310
14259
EN
FS
ANORTHOSITIC
GABBRO
OLIVINE
SPINEL
90
80
FORSTERITE
FAYALITE

Fig. 10